# Sediment pathways and morphodynamic response to a multi-purpose artificial reef – New insights

# Sediment pathways and morphodynamic response to a multi-purpose artificial reef – new insights

*Vieira da Silva, Guilherme [a], Hamilton, Daniel [b], Strauss, Darrell[a], Murray, Thomas[a], Tomlinson, Rodger[a]*

*[a] Coastal and Marine Research Centre Room 2.01, Building G51 Griffith University Gold Coast Campus, Queensland, 4222, Australia*

*[b] City Assets, Transport and Infrastructure, City of Gold Coast, 833 Southport - Nerang Rd, Nerang QLD 4211 Australia*

*Corresponding Author: Guilherme Vieira da Silva (g.vieiradasilva@griffith.edu.au)*

**Abstract**

Multi-purpose Artificial Reefs (MPARs) are structures that may provide aesthetically acceptable coastal protection and improve recreational outcomes. Twenty years after construction of the first MPAR, Narrowneck reef on the Gold Coast of Australia, most of the available literature is still focused on the planning, design and construction of such structures and peer-reviewed publications on their post-construction monitoring, interaction with sediment transport and impacts on coastal morphology are lacking. The aim of this paper is to evaluate how does Narrowneck reef influence the sediment transport, and morphological changes around the anthropogenic structure, two decades after construction. To do so, a combination of ten high spatial resolution topo-bathymetric surveys from the top of the dune to the 10 m depth captured over 21 months and a series of 60 simulations using a calibrated numerical model were used. Our results demonstrate that: although not expected during design or reported in similar structures, sand can bypass the MPAR around its offshore end; under oblique waves, the longshore currents are deflected as they pass the reef, resulting in a shadow zone on the downdrift side where sand deposits; the bar crest tends to be higher on the reef's updrift side compared to downdrift, indicating that the MPAR can act as a store for sediments, as initially designed. Furthermore, the MPAR can act to stabilise the bar as it moves onshore with a downdrift offset of the inner bar as a result of low oblique wave incidence. The results presented here demonstrate that the short-term response to the MPAR twenty years after construction is more closely related to the deflection of longshore currents as they encounter the reef than to the dissipation of wave energy. This is because MPARs are designed to dissipate just enough wave energy so that they can achieve their recreational goal (surfing).

**Keywords***: bar morphology, erosion, beach protection, adaptation, MPAR, multifunctional reefs.*

## 1 INTRODUCTION

Sandy beaches are highly dynamic and these coastlines experience erosion and accretion events over a wide range of time scales (Short and Trembanis, 2004). However, despite the highly dynamic nature of sandy coasts, many coastal cities have been constructed within the region of natural variability of the beach and experience extreme erosion and property loss. Moreover, some locations experience long-term trends in coastal erosion. These factors often result in coastal protection strategies such as beach nourishment and the construction

of seawalls as a last line of defence (Tomlinson et al., 2016; Sinay and Carter, 2020; Toimil et al. 2020). In some cases, severe erosion has led to the relocation of residents (Correa and Gonzalez, 2000; Abel et al., 2011). Climate change projections (Pörtner et al., 2019) are predicted to affect the future wave climate (Hemer et al., 2013; Wang et al., 2014; Camus et al., 2017; Young and Ribal, 2019) which has the potential to further impact coastal areas (Ranasinghe et al., 2016) due to anticipated changes in longshore sediment transport (Sierra and Casas-Prat, 2014) and chronic erosion (Greenslade et al., 2020) resulting in an increase in coastal protection works. Ware et al. (2020) highlights that the cost related to the implementation of coastal protection varies significantly depending on the adopted representative concentration pathways (RCP – Pörtner et al., 2019). While relocation of coastal cities is challenging (Abel et al., 2011; Grace and Thompson, 2020), construction of structures such as groynes and seawalls that may help to stabilise the coastline tend to have a negative visual amenity impact and can potentially cause severe downdrift erosion (van Rijn, 2011). On the other hand, beach nourishment has the benefit of increased beach amenity (i.e. recreational width) and enhances the storm buffer. However, nourishment of the visible upper beach needs to be maintained more regularly than coastal protection strategies using hard structures. Antunes do Carmo (2019) suggests that multifunctional structures such as multi-purpose artificial reefs (MPARs) are a good option for coastal protection. These structures stay submerged with no negative visual impact, they can be used in combination with beach nourishment to act as a store for sediment and increase the lifetime of the nourishment deposition with the added benefit of enhancing biodiversity and recreation opportunities.

Initial studies by Walker et al. (1972) suggested that artificial surfing reefs could be created and be associated with other benefits such as coastal protection. The first MPAR designed for coastline protection and improved surfing conditions was constructed in between 1999 and 2000 at Narrowneck, Australia (Black, 2001; Jackson, 2001; Turner et al., 2001). To date only a few other similar structures have been designed and constructed with the same functional purpose (Mead and Black, 1999; Taranaki Regional Council, 2009; Mead et al., 2010; Atkins, 2010; Yardley et al., 2012; Mortensen et al, 2015). There is no consensus in the literature regarding the construction of these structures and the ones that have been constructed vary in terms of material, construction methods and dimensions. Their impact on surrounding morphology and sediment transport is hard to assess as the published data (particularly in peer-reviewed journals) on their monitoring programs is limited. As a result, there are divergent opinions within the community as to the operational success of these engineering solutions and the claimed success of some of these structures is controversial (Ranasinghe et al., 2006; Jackson and Corbett, 2007; Blacka et al., 2013; Ng et al. 2013,

2015, López et al., 2016). Ranasinghe and Turner (2006) indicated that most of the submerged coastal structures that they analysed revealed erosion in the lee of the structure. Additionally, it has been shown that artificial reefs respond differently than emergent offshore breakwaters with most of the morphological impact of the reefs being observed underwater (Vieira da Silva et al., 2020). To our knowledge, no study to date has conducted or reported on successive bathymetric surveys with enough frequency and spatial density to capture the morphological changes around a MPAR and linked them to different environmental conditions. Moreover, no calibrated numerical modelling study of MPAR-related morphological response has been reported following a MPAR construction. The data collected around the first MPAR (i.e. Narrowneck reef) provides a unique opportunity to better understand the impacts of such structures on sediment transport pathways and surrounding morphology. Therefore, the aim of this paper is to evaluate how the MPAR affects the sediment transport, and morphological changes around it twenty years after construction.

### 1.1 Regional Setting / Study Area

The study area is located on the northern beaches of Gold Coast, Australia (Figure 1) within the Surfers Paradise stretch of open ocean coastline, the premier coastal tourist beach in Australia (Short, 2000). Here, the Nerang River meanders and is separated from the ocean by a 100-150 m isthmus of sand (known as Narrowneck). To the north of Narrowneck, a residual relict delta remains from the historical northward migration of the Nerang River. This deposit is reported to currently supply a locally higher volume of sand via onshore transport as the feature tends toward a new equilibrium (Patterson, 2007; Patterson and Nielsen, 2016). The sand is fine with $d_{50}$ of 0.2 mm (Castelle et al., 2009) and the region is subject to a semi-diurnal and micro-tidal regime, with maximum tidal range of up to 2.1m with a mean range of 1 m (Kobashi et al., 2014). The coast is exposed to moderate to high waves ($H_s$ at 70 m depth can be higher than 7 m) with significant seasonal variability. The north end of the coast here is exposed to all swell directions (Vieira da Silva et al., 2018a). Climatic indices are linked to variability in the longshore sediment transport in the region (Splinter et al., 2012; Silva et al., 2021). Extreme erosion has been recorded in the area since the early 1900's leading to a series of measures to protect the area and prevent the breakthrough of the Nerang River to the ocean at Narrowneck (Table 1). These measures range from the construction of a timber wall to prevent further erosion in 1923 (upgraded in 1967 to a boulder wall – known as the A-line), to the development of the Northern Gold Coast Beach Protection Strategy in 1997 (Boak et al., 2000; Jackson, 2001). The strategy included the nourishment of the northern beaches with 1.3 $Mm^3$ of sand and the construction of a submerged reef at Narrowneck to help stabilise the nourishment and improving surfing

conditions (Black, 1999; Jackson, 2001; Turner et al., 2001). The reef was designed to provide a coastal control point assisting the maintenance of Surfers Paradise beach and, after achieving its new equilibrium, no more than approximately 80,000 $m^3$/year of nourishment would be required downstream (Black, 1999). To do so, field measurements were conducted in the area (Hutt et al, 1999) which supported both the numerical (Black, 1999) and physical modelling of the reef (Turner et al., 2001).

The subaerial beach at the study site was nourished in 1999 followed by the construction of Narrowneck reef. The reef was constructed using 408 large sand filled geotextile containers 20 m in length that ranged from 3 to 4.5 m in diameter with an overall volume of 60,000 $m^3$ (Jackson et al, 2007). It is located between the -2 m AHD (Australian Height Datum - AHD, which is equivalent to the mean sea level) contour (to allow sediment bypassing between the shoreline and the reef) to -10.4 m AHD (Black, 1999). The reef extends 200-350 m alongshore and 400-500 m cross-shore (Jackson and Hornsey, 2002; Ranasinghe and Turner, 2006). The reef crest was initially designed to be at -0.67 m AHD (Black and Mead, 2001) however, due to safety concerns and to avoid possible excessive sand retention the crest height adopted was -1.5 m AHD (Jackson et al., 2007). The reef construction occurred after an erosive storm swell event which reset the morphology to an offshore Longshore Bar and Trough beach state (Jackson et al., 2007). As the bar on which the Narrowneck reef construction began migrated shoreward, the crest lowered and so the reef was periodically topped up in subsequent years. Due to safety concerns, the crest was lowered to -2.5m AHD to reduce the frequency of hazardous waves for surfers and to avoid the *sucking dry* or draining of water off the artificial structure, which is commonly observed at natural surf zone reefs during low tides (Jackson et al., 2007). Moreover, under small wave conditions that do not break on the reef, significantly more surfers have been reported in the lee of the reef (Jackson et al., 2007). After the latest reef top-up, completed in 2018, multibeam survey indicates that the reef crest is currently at -2.2 m AHD.

Performance of the reef in terms of coastal protection is considered ‘good’ (Jackson et al, 2007; Jackson et al., 2012; Ng. et al, 2013; Ng. et al., 2015) with beach accretion reported (Ranasinghe and Turner, 2006). Formation of a shoreline salient inshore of the reef was also reported under some conditions (Jackson et al, 2007) but it has not been consistently observed over the mid to long term (i.e. 20 years). The largest impact of the MPAR over the long-term has occurred in the nearshore with sand accumulation updrift of the reef (Vieira da Silva et al., 2020). Instruments deployed by the authors measured waves and currents around the reef indicating that the reef tends to attenuate waves higher than 1.5 m ($H_s$) while an increase in height of waves less than 1.5 m $H_s$ (shoaling) is observed over the reef. Moreover, the longshore currents are deflected, indicating possible sediment pathway

changes. Surfing conditions were also reported to have improved with increased wave breaking both at the reef and inshore of the reef under smaller conditions (Turner et al., 2004; Jackson et al, 2007) although not as initially predicted (Black and Mead, 2001). Jackson et al. (2007) reports that public perception regarding surfing conditions were largely negative for few reasons: a) due to the existence of several nearby world-class surfing breaks; b) the distance of the take-off area from the beach (300 m offshore) and the frequent presence of waves inshore of the reef and c) negative press statements even before the reef's completion. A positive aspect of the Narrowneck reef refers to the ecological impact it had with attraction of several species resulting in increased fishing and diving (Jackson et al, 2012; Ng. et al., 2015).

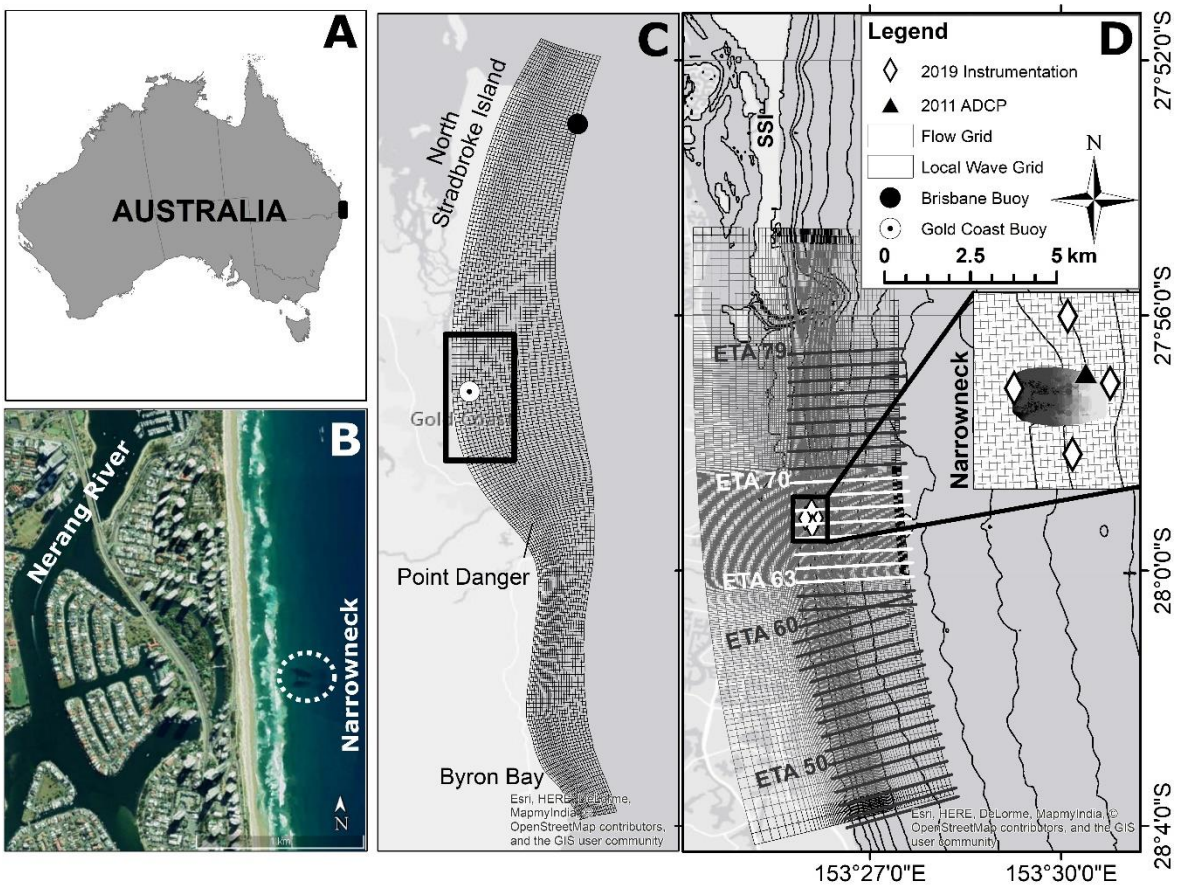


**Figure 1: A) Rectangle indicates the location of the study area; B) Google Earth image displaying the location of the reef; C) Regional grid and locations of the wave buoys; D) Local grids, the Narrowneck reef, location of instruments used for model calibration and the main survey lines (ETAs).**

**Table 1: Narrowneck events chronology – Source: Coastal and Marine Research Centre Knowledge Hub.**

| Date | Key Event |
|---|---|

| | |
|---|---|
| 1923 | Timber seawall constructed at Narrowneck (up to 35m seaward of the general seawall alignment) to protect the highway |
| 1954 (Feb) | 'The Great Gold Coast Cyclone' |
| 1967 (Jan - May) | Tropical cyclones Dinah, Barbara, Dulcie, Elaine and Glenda >100-year event. |
| 1967 | Construction of boulder wall at Narrowneck |
| 1970 (Dec) | The Delft Report – the basis for coastal protection works and investigations on the Gold Coast - guided Gold Coast beach management > 30 years |
| 1974 (Mar) | Tropical cyclone Zoe |
| 1974 | Beach nourishment (Main Beach to southern Surfers Paradise) (1.5Mm$^3$) |
| 1985 | Sand nourishment works (300,000 m$^3$,Narrowneck) (142,000 m$^3$, Surfers Paradise) |
| 1990's | Decrease in beach width; exposure of boulder wall at Narrowneck |
| 1993 | Proposal - Artificial headland (75m) for Narrowneck |
| 1997 | Northern Gold Coast Beach Protection Strategy (NGCBPS) initiated |
| 1998 | Design studies – Investigation of the reef design for: sediment transport (including sedimentation patterns, net littoral sediment drift, and effects on adjacent beaches); surfing amenity; and the field measurement program ([University of Waikato & National Institute of Water and Atmospheric Research (NIWA)] |
| 1999 | Design studies – Physical model study (1:50 scale model) [Water Research Laboratory (University of New South Wales)] |
| 1999 | Northern Gold Coast Beach Protection Strategy (NGCBPS)implemented |
| 1999 (Feb – Jun) | Sand nourishment works (1.1 million cubic meters – upper beach) |
| 1999 (Aug – Dec) | Construction - Artificial reef |
| 2000 | Sand nourishment works (Surfers Paradise) / completion of reef |
| 2002 | Container 'top-up' & replacement |
| 2004 | Container 'top-up' & replacement |
| 2006 | Container 'top-up' & replacement |
| 2009 | Significant storms (1:10 ARI) |
| 2011 | Underwater condition survey |
| 2012-2013 | Removal of ~10,000m$^3$ of sand from the dunes at Narrowneck to restore the beaches at Surfers Paradise. |
| 2013 | Tropical cyclone Oswald |
| 2017 | Design studies – modelling of 2 reef renewal options.[International Coastal Management (2017)] |
| 2017 (Sep) | Commencement of reef renewal (top-up) |
| 2017 (Jun-Sep) | Large-scale nearshore nourishment (over 3 million cubic metres - nearshore) |
| 2018 (Jun) | Completion of reef renewal (top-up). |
| 2019 (Feb) | Tropical cyclone Oma |

## 2 MATERIAL AND METHODS

To achieve the aim of this paper, the methods were divided into two parts: a) high spatial and temporal topo-bathymetric dataset analysis and; b) numerical modelling. Each part is described below in detail.

### 2.1 Topo-bathymetric surveys

Topo-bathymetric surveys were carried out in the area of interest from the top of the dune to the -10 m contour (AHD) between the historically named 'ETA lines': ETA 63 and ETA 70 (see **Figure 1**) with alongshore distance between the survey lines varying between 25 and

50 m. In total, ten surveys have been carried out over 21 months, the first on the 19th July 2018 and the most recent on 23rd April 2020. The upper beach measurements were conducted around low tide using a RTK-GPS while the sub-tidal region was provided by the City of Gold Coast and used a single beam echo-sounder and RTK-GPS. The nearshore survey is weather dependent and ideally happens during low-wave, low-wind and high tide range. Each survey was then interpolated on to a regular grid (2x2 m) so that the bars, trough and rip channels were well represented. Successive surveys were compared to quantify morphological changes around the reef driven by environmental conditions between surveys and the evolution of the upper beach volume was calculated. The beach profiles at the main ETA lines (ETA 63 to ETA 70) are presented in the supplementary material to support the analysis and the offshore (Brisbane buoy, at - 70 m AHD) and nearshore (Gold Coast buoy, at - 17 m AHD) wave data (see location in Figure 1) were used to help with the interpretation of the data.

Despite the usefulness of the dataset collected in interpreting the morphological changes in the region and inferring some sediment transport pathways around the MPAR, the data has limitations. In some cases, due to the difficulties of surveying the nearshore region, the interval between surveys is large and encompasses multiple high wave energy events and therefore it is not possible to differentiate the transport patterns related to a single event. Moreover, the dataset does not cover all types of events that could happen in the region. Therefore, numerically simulating key scenarios would provide useful information to fill gaps in the measured dataset.

## 2.2 Numerical modelling

Numerical modelling provides a detailed understanding of the currents, waves and sediment transport that led to the morphological changes observed in the dataset. To do so, the model chosen was Delft3D (Lesser et al., 2004). Delft3D is considered state-of-the-art in terms of morphological simulations of complex coastal processes such as waves, hydrodynamics, sediment transport and morphological changes (Lesser et al., 2004). The present paper used the wave (SWAN - Booij et al., 1999; Ris et al., 1999) and flow (including sediment transport and morphology) modules running online. This means that waves generate currents that would generate sediment transport that would change the morphology that then would affect the wave propagation in a feedback process. This feature (online simulation) is particularly relevant to the simulation of morphological changes where the feedback process is crucial to obtain realistic results such as during morphological calibration of the model.

### *2.2.1 Grids and Bathymetry*

The wave model used in this paper is based on the wave model presented by Vieira da Silva et al. (2018a). The model domain spans the east coast of Australia from North Stradbroke Island, QLD to Byron Bay, NSW increasing its resolution shoreward (Figure 1). The largest grid provides a relatively coarse bathymetry for propagation of waves from deep water and the smallest grid resolves shallow water features in progressively more detail.

The large grid has 221 × 25 elements and resolution of approximately 700 × 600 m. The local grid differs from the one presented by Vieira da Silva et al. (2018a) to better represent Narrowneck and the associated bars. It has 306 × 107 elements and resolution varying from 120 × 250 m to 20 × 20 m. The flow grid is similar to the detailed wave grid, being one row smaller to avoid numerical problems and has 5 vertical sigma layers (quasi-three dimensional – Q3D).

Samples used to establish the nearshore bathymetry and upper beach topography consists of the data described above. For the morphological calibration, the initial bathymetry was taken from the survey of the 2nd August 2018, while scenarios were simulated for accreted (12th September 2018) and eroded (26th March, 2019) conditions to understand the role of the underlying bathymetry on sediment transport under different conditions. The offshore part of the grid bathymetry was completed using data from Project 3DGBR (Beaman, 2010).

### *2.2.2 Waves and Flow Calibration and Validation*

The boundary conditions consisted of waves measured at the Brisbane Waverider buoy, with water levels and winds measured at the Gold Coast Seaway. The wave and flow models were calibrated using the dataset presented by Vieira da Silva et al. (2020) which consisted of a series of instruments deployed around Narrowneck reef (see Figure 1 and Table 2). For more details on deployment and instrument configuration, refer to Vieira da Silva et al. (2020).

**Table 2: Instruments used for numerical model calibration.**

| Instrument | Deployment period | Location | Depth |
|---|---|---|---|
| ADCP Linkquest Flowquest 1MHz | 14th March 16th April 2019 | South of the Reef | 7.5 m |
| ADCP Linkquest Flowquest 1MHz | 14th March 16th April 2019 | North of the Reef | 5.5 m |
| Spoondrift Spotter | 14th March 16th April 2019 | Offshore | 10 m |
| RBR | 14th March 16th April 2019 | Offshore | 10 m |
| RBR | 2nd to 7th to April 2019 | Inshore | 5.5 m |
| ADCP Sontek Argonaut 3 MHz | 2nd to 7th to April 2019 | Inshore | 5.5 m |

The instruments above were used to calibrate the model that was then used to simulate a separate validation period between April and May 2011 when wave and current data was collected at a depth of approximately – 7m (AHD) (see Figure 1). The dataset for validation was provided by the City of Gold Coast and consists of one ADCP deployed near Narrowneck to measure waves and currents (Stuart and Lewis, 2011).

### *2.2.3 Sediment Transport and Morphological Calibration*

Sediment transport modelling is challenging, and transport formulations often contain multiple parameters that are used to calibrate the formulations if measured data is available. Therefore, the simple application of a sediment transport formula without model calibration can lead to results that differ significantly from observations. Measurements of sediment transport in the active zone of the profile are quite challenging (e.g. Kraus, 1987; Vieira da Silva et al., 2016) and are often measured at a single (or very few) points. Due to the hostile nature of the surf zone instruments may become buried while retrieved data may be non-existent or unreliable due to instrument movement. To overcome these challenges, this paper used the morphological changes (differences in bed level between surveys) as proxy for sediment transport (i.e. we considered that if the morphological changes are well represented by the model between surveys then so should the sediment transport be well represented). Moreover, morphological changes are measured over a longer period compared to an instantaneous in-situ sediment transport experiment, therefore also spanning a wider range of conditions. To do so, the morphological changes were evaluated during the calibration period and the wave model was driven with Brisbane Waverider Buoy data at the offshore boundaries. The flow model was forced with observed water levels (at the offshore boundary) measured at Gold Coast Seaway, 5 km north of the study area (provided by the Queensland Government) and winds (spatially uniform over the domain) measured at Gold Coast Seaway (provided by the Bureau of Meteorology, Australia) and the Neumann condition was applied to the lateral boundaries. The simulation was started on 2$^{nd}$ August 2018 and ended on 12$^{th}$ December 2018 and included a relatively calm period followed by an easterly swell event. As for waves and hydrodynamic modelling, a series of sensitivity tests and calibration runs were carried out to obtain the best transport formulation and corresponding set of model parameters that resulted in the best reproduction of the observed morphological changes.

Two types of morphological calibration were carried out: 1) the measured shoreline change was compared to the model results and the errors were assessed by the root mean square error (RMSE) at the ETA lines and; 2) the morphological change results from the model at the interest area (from the dune to -10 m AHD between ETA 63 and ETA 70) were compared to the measured morphological changes and the Brier Skill Score (BSS) was used to assess the 'goodness' of the calibration. BSS has been increasingly used by coastal researchers to assess the skill of coastal process models (Sutherland et al. 2004; Roelvink et al. 2009; Vousdoukas et al. 2012; Simmons et al., 2017). It compares the measured changes with the modelled changes and values = 1 represent perfect agreement. van Rijn et al (2003) classified Brier Skill Score according to: BSS <= 0: bad; 0 < BSS <= 0.3: poor; 0.3

< BSS <= 0.6: reasonable / fair; 0.6 < BSS <= 0.8: good; and 0.8 < BSS <= 1: excellent. The BSS is calculated as follows (eq.02):

$$BSS = 1 - \frac{\sum(z_{mod} - z_{meas})^2}{\sum(z_0 - z_{meas})^2} \quad \text{(eq.02)}$$

where $z_0$ is the initial measured profile, $z_{mod}$ is the final model result, $z_{meas}$ is the final measured profile.

Following the calibration of the model, it was possible to simulate a variety of scenarios with increased confidence to support the measured dataset and to support the understanding of the interaction of the MPAR with the sediment transport and morphological changes in its surrounding areas.

*2.2.4 Scenarios simulation*

A series of 60 scenarios were simulated to aid understanding of the sediment transport pathways around the MPAR. To select the wave cases the complete time series was divided into eight directional bins covering the main wave directions. For each direction two wave heights were chosen, a median significant wave condition ($Hs_{Q50\%}$) for each direction and an extreme wave for that direction, the $Hs_{Q99.86\%}$ for each direction, which is analogous to the $Hs_{12}$ (i.e. the wave height that is exceeded 12 hours per year). Wave directions that propagate offshore (southwest, west and northwest) were not simulated. The associated wave period was defined following Kamphuis (2010). The scenarios were simulated over two different initial surveyed bathymetries: an accreted beach (12th September 2018) and an eroded beach (23rd June 2019). Moreover, simulations were carried out at 0 m AHD, low tide (-0.9 m AHD) and high tide (0.9 m AHD) so that the influence of the beach state and tide levels on sediment transport pathways could be assessed.

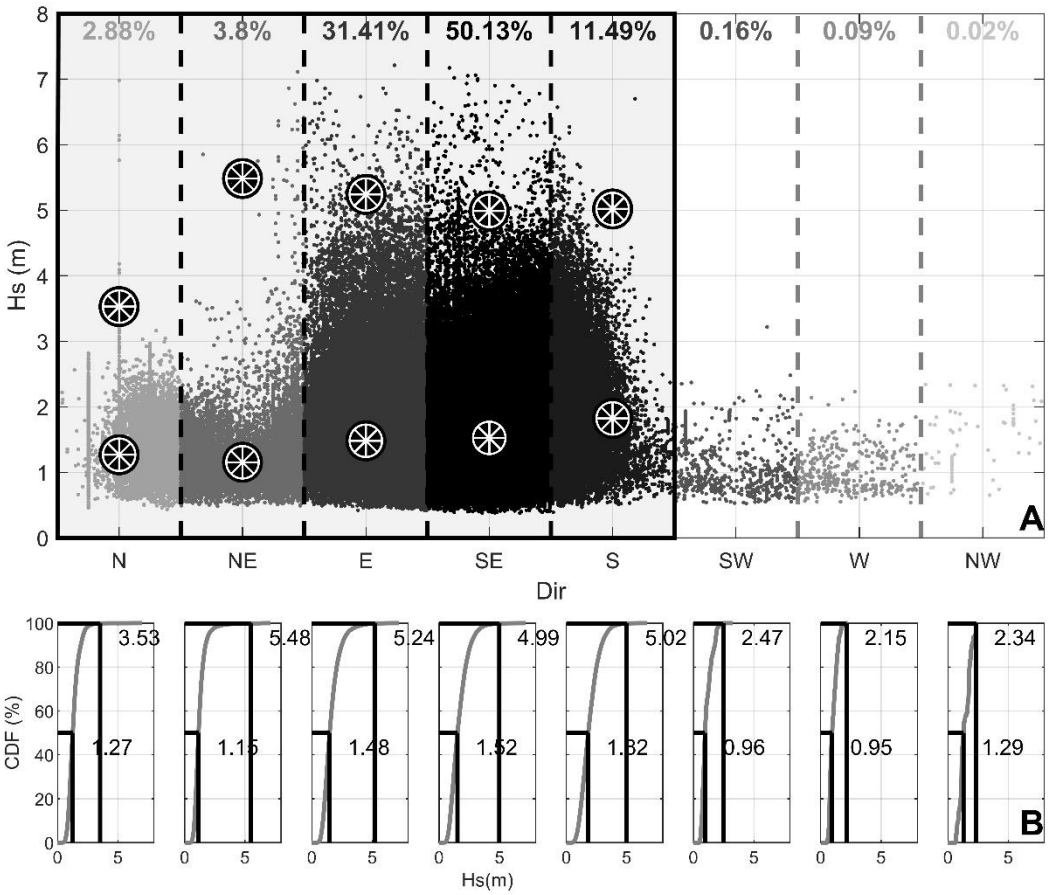


**Figure 2: Selected wave cases for each wave direction. $Hs_{Q50\%}$ and $Hs_{Q99.86\%}$ - significant wave height exceeded 50 and 98.86% of the time, respectively. A) scatter plot of waves and selected wave cases; B) cumulative distribution function for each direction with values representing the $Hs_{Q50\%}$ and $Hs_{Q99.86\%}$ per direction. Waves to SW, W and NW were not simulated as they propagate offshore.**

The sediment transport results from the model were analysed at cross sections along the model domain (from ETA 63 to ETA 70 – see Figure 1). Moreover, the model results for waves, currents and sediment transport are presented in the area of interest to support the findings and aid the understanding of sediment transport pathways in the area.

## 3 RESULTS

Results are divided into two sections: topo-bathymetric surveys and numerical modelling which are described in detail below.

### 3.1 Topo-bathymetric surveys

Digital elevation models (DEMs) of the surveys captured between 19th July 2018 and 23rd April 2020 are presented in Figure 3 while Figure 4 presents the difference in elevation between successive surveys and the evolution of the upper beach volume. The DEMs were used to classify the beach morphodynamic state according to Wright and Short (1984). The

beach profiles across the ETA lines over time as well as the environmental conditions during the study period are presented in the supplementary material with the vertical lines representing dates of surveys.

The period between the first (19th July 2018) and the third (17th August 2018) surveys was characterised by low energy recovery period with the beach transitioning from rhythmic bar and beach (RBB) to transverse bar and rip (TBR). During this period, the highest upper beach accretion is observed shoreward of Narrowneck reef (Figure $4_j$), whereas the beach both north and south of the reef presented lower rates of accretion, this is mainly due to the fact that behind the reef the bar is in close proximity to the upper beach and beginning to merge to the shoreline.

Following this, the next two surveys (12th December 2018 and 23rd March 2019) depict a strong erosional period (Figure $3_{5,6}$, Figure $4_{d,e}$). During this period a series of events with moderate energy occurred, with the most significant ones being: an event in October 2018 and Tropical Cyclone Oma (TC Oma) in March 2019.

The first event reached 4.5m ($H_s$) and reset the nearshore morphology to a longshore bar and trough (LBT) and the inner bar presented a RBB state transitioning towards a TBR state. A longshore bar formed in alignment with the inshore part of Narrowneck reef, (i.e. the bar is approximately the same distance offshore as the inshore edge of the reef), particularly towards the south of the reef (400 m to the south of the reef) (Figure $3_5$). North of the reef the longshore bar crest only appears 700 m downdrift. A sand accumulation attached to the northeast part of the reef is also revealed between the -6 to -8m (AHD) depth contours. The difference between surveys (Figure $3_d$) demonstrates that cross-shore sediment transport occurred during the higher energy events with the bar aligned with the shoreward part of the reef. An increased accumulation of sand is observed in the north part of the reef area while the greatest upper beach erosion is located inshore of the reef (Figure $4_{d,j}$), possibly due to the lower crest of the outer bar at this location compared to further north and south of the reef (Figure $3_5$) resulting in less attenuation of the easterly waves at this location.

Tropical Cyclone Oma also reached $H_s$ of 4.5 m recorded on the Gold Coast buoy. Compared to the October event, TC Oma sustained significant wave heights above 1.5 m for approximately 10 days as opposed to 6 days for the October event, $H_s$>3 m lasted 3 days during TC Oma and 2 days during the October event yet both events were considered to be 1 in 4 year events (with respect to wave height). Furthermore, TC Oma increased the water levels (see supplementary material) and induced increased levels of coastal erosion. Following TC Oma, the bar moved further offshore and extended to join the reef (Figure $3_6$). The increased deposition of sand particularly on the north side of the reef indicates the

possible sand bypassing pathway. Due to TC Oma's wave direction (from southeast) a strong longshore current formed transporting significant amounts of sand northwards and offshore leading to scouring of the beach. During TC Oma little longshore variation of the upper beach erosion was observed (Figure $4_{e,j}$) due to the strong longshore currents that formed. Under these very energetic southeast wave conditions the width of the longshore bar increased allowing the sand suspended by these conditions to be transported around (offshore of) the reef by the current.

Then, the period following TC Oma was mostly a recovery period with relatively low waves and onshore transport of sand. The survey of 14th June 2019 (Figure $3_7$) shows a depression inshore of Narrowneck reef as a discontinuity in the longshore bar as a result of the lack of sand able to migrate onshore at this location due to the presence of the reef. As the sand continues moving onshore, it appears that the MPAR plays a particularly important role in controlling the morphodynamics of the region with the bars in the immediate vicinity of the reef moving onshore, whilst the nearshore bar further to the north and south of the reef are more detached (Figure $3_8$). Moreover, Figure $3_9$ indicates that both updrift and downdrift of the MPAR (between ETA 66 and 68) the depth contours between around -5 to -9 m (AHD) are further offshore compared to the rest of the survey (south of ETA 66 and north of ETA 68), indicating that under these conditions the reef can help to hold sand in its surroundings.

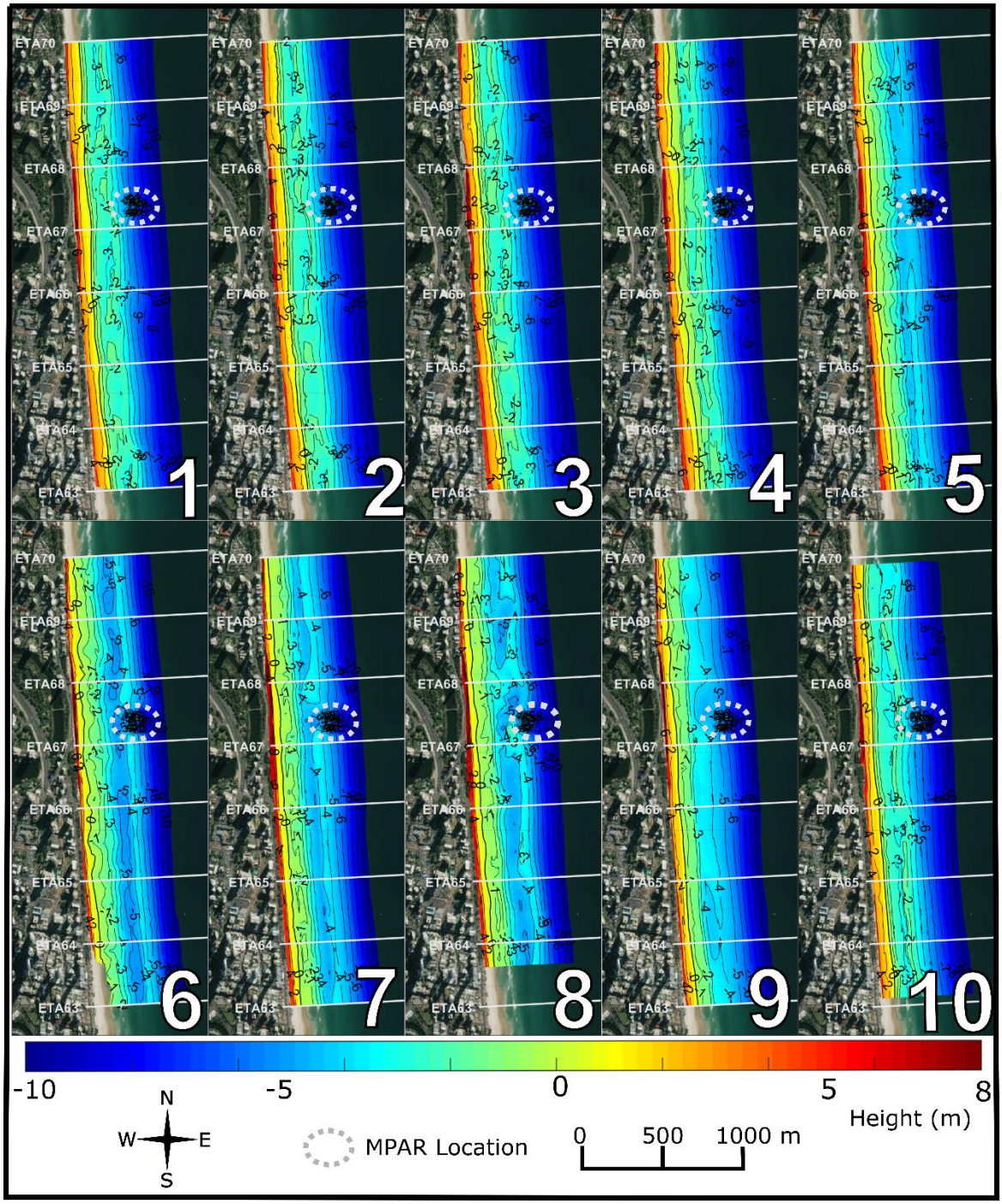


**Figure 3: Topo-bathymetric surveys. 1) 19th Jul 2018, 2) 2nd Aug 2018, 3) 17th Aug 2018, 4) 12th Sep 2018, 5) 12th Dec 2018, 6) 23rd Mar 2019, 7) 14th Jun 2019, 8) 24th Jul 2019, 9) 5th Dec 2019, 10) 23rd Apr 2020.**

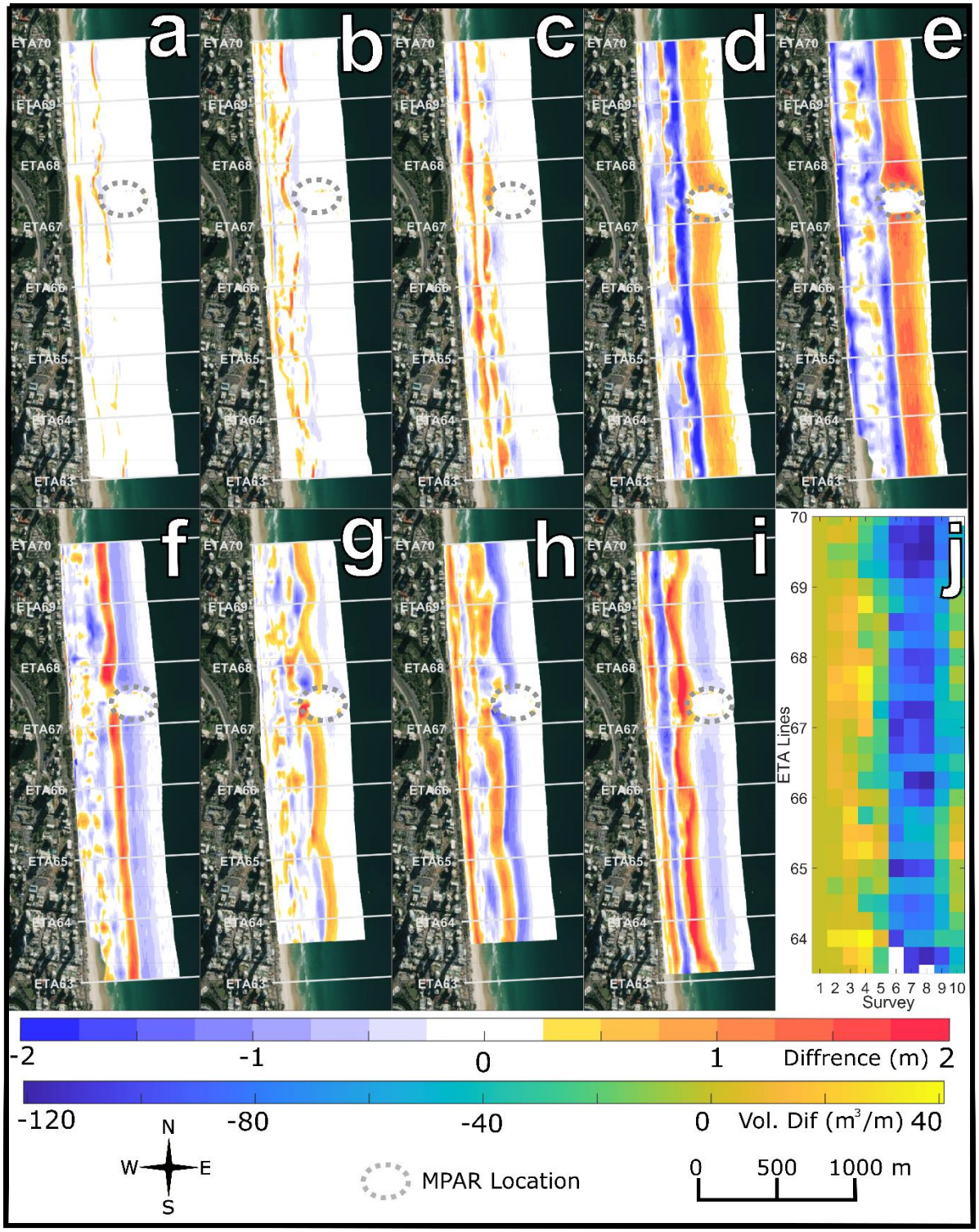


Figure 4: **Differences between successive surveys. a) 19th Jul 2018 to 2nd Aug 2018, b) 2nd Aug 2018 to 17th Aug 2018, c) 17th Aug 2018 to 12th Sep 2018, d) 12th Sep 2018 to 12th Dec 2018, e) 12th Dec 2018 to 23rd Mar 2019, f) 23rd Mar 2019 to 14th Jun 2019, g) 14th Jun 2019 to 24th Jul 2019, h) 24th Jul 2019 to 5th Dec 2019, i) 5th Dec 2019 to 23rd Apr 2020, j) upper beach volume ($m^3$) change through time (x axis) from initial profile (19th Jul 2018) along the study area (y axis). Values above (below) zero indicate upper beach volume higher (lower) than the first survey.**

### 3.2 Numerical modelling

The quality of model results is directly related to the quality of the input data and the available data for calibration. Thus, while uncalibrated models can be used as a first pass assessment, good quality field data is crucial to reliably simulate coastal processes. The calibration results are presented for waves, hydrodynamics and morphological changes followed by the results for the main sediment transport scenarios.

### *3.2.1 Model Calibration and Validation*

The key wave and hydrodynamic parameters that resulted in the best representation of the measured data are presented in Table 3.

**Table 3: Delft 3D wave and flow models key calibration parameters and activated processes.**

| | Parameter | Value |
|---|---|---|
| Wave model | Depth-induced Breaking | Alpha = 1; gamma = 0.73 |
| | Bottom Friction | 0.067 $m^2 s^{-3}$ |
| | Diffraction | activated |
| | Whitecapping | activated |
| | Refraction | activated |
| | Frequency shift | activated |
| Flow model | Wind drag (breakpoints: coefficient / wind speed | A: 0.00063 / 0 m $s^{-1}$<br>B: 0.00723 / 100 m $s^{-1}$ |
| | Bottom roughness (Chézy) | U = 45 $\sqrt{m}s^{-1}$ / V = 45 $\sqrt{m}s^{-1}$ |
| | Roller model | Activated |

The model calibration together with the RMSEs are presented in Figure 5 for the instruments deployed north and south of Narrowneck reef and offshore and inshore of the reef (see Figure 1 for location of instruments). The results indicate a good agreement between the model and the measurements at various locations. The same model was used to simulate a different period (validation) to increase model confidence – results are presented in Figure 5 (far right column). Once again, the figures demonstrate that the model is in good agreement with the measured data.

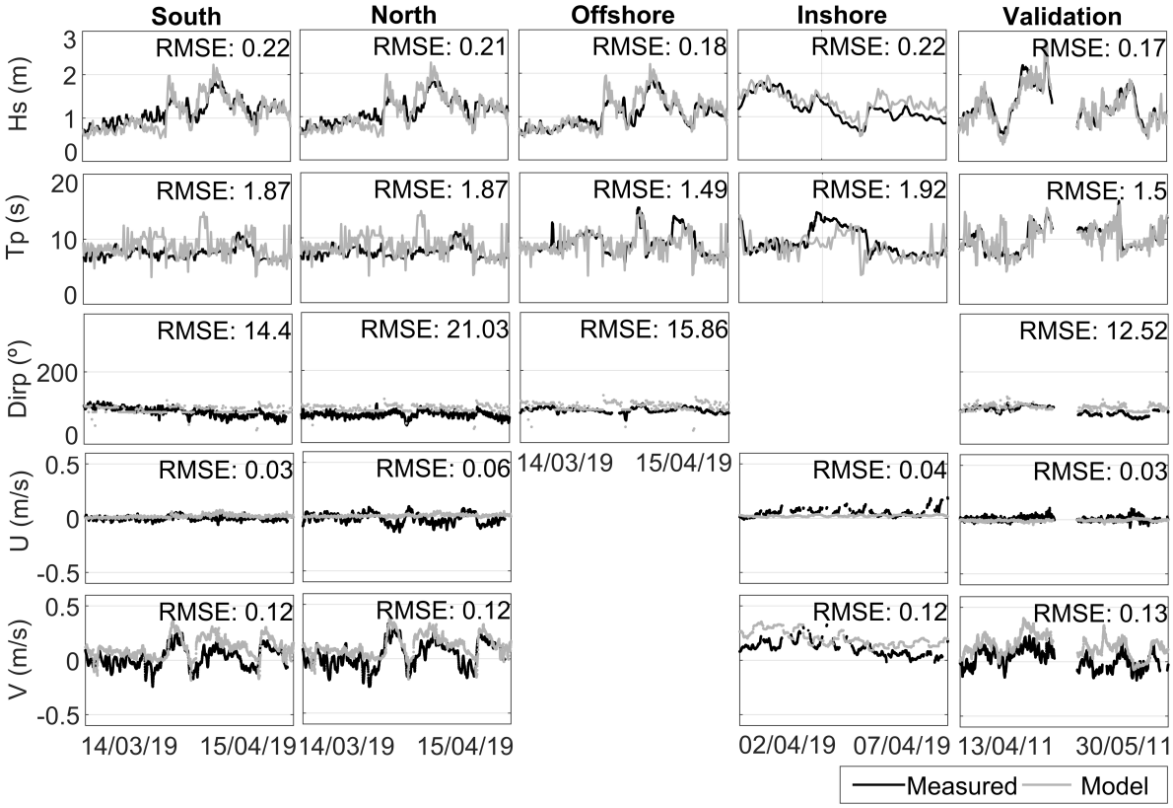


**Figure 5: Model calibration for the ADCPs deployed north and south of Narrowneck reef (columns 1-4) and validation for ADCP deployed in 2011 (far right column). Black lines are the measured data and grey lines are the model results.**

*3.2.2 Morphological Calibration*

Calibrating coastal area morphological models is more challenging than calibrating hydrodynamic and wave models because: 1) morphology changes are based on sediment transport formulas that were mainly developed for different environments; 2) morphological models rely on accurate representation of waves and hydrodynamics and errors in these processes propagate to the resulting morphological changes and; 3) small errors in sediment transport calculations will accumulate over time and will result in poor morphologic calibration. Nonetheless, a good calibration of a morphological model, when achieved, provides a quantification of errors that allows a better interpretation of the results and understanding of the model limitations as well as providing increased confidence compared to an uncalibrated model.

The model calibration process indicated that the Van Rijn et al. (2000) transport formula best reproduces the morphological changes observed at the study site and the adopted parameters are described below.

**Table 4: Key parameters adopted for morphological calibration.**

| Parameter | Value |
|---|---|

| | |
|---|---|
| Reference height factor | 1 |
| Threshold sediment thickness | 0.05 |
| Estimate ripple height factor | 2 |
| Factor for erosion of adjacent cells | 1 |
| Wave-related suspended sediment transport factor | 0.1 |
| Wave-related bed-load sediment transport factor | 0.1 |

419

420 Figure 6 presents the measured morphological changes (left) together with the modelled
421 changes (centre) and the shoreline changes (right). The full surveyed area is well
422 represented by the model with a BSS of 0.6, which is considered reasonable/good according
423 to van Rijn *et al.* (2003). Moreover, the morphological changes and bar movements are
424 qualitatively very well reproduced by the model (Figure 6). The offshore transport of sand is
425 clearly identified in both the measurements and the model results. A wider bar, however, is
426 formed in the simulations compared to the measurements. The measured data also
427 indicates onshore sediment transport from offshore (depths between 8-10 m) to the bar
428 (around 6 m) which is not well represented by the model. This is expected as the onshore
429 migration of bars is still poorly understood and the physics concerning this process is not
430 well-reproduced by the models. Nonetheless, a good morphological model calibration and
431 reproduction of the correct patterns in terms of morphological changes indicates that the
432 sediment transport process is well represented around Narrowneck reef. Shoreline changes
433 are quite well represented with RMSE of 7.57 m, which is less than half the size of a grid cell
434 and, therefore, considered excellent. Therefore, the models provide good confidence to
435 simulate sediment transport scenarios.

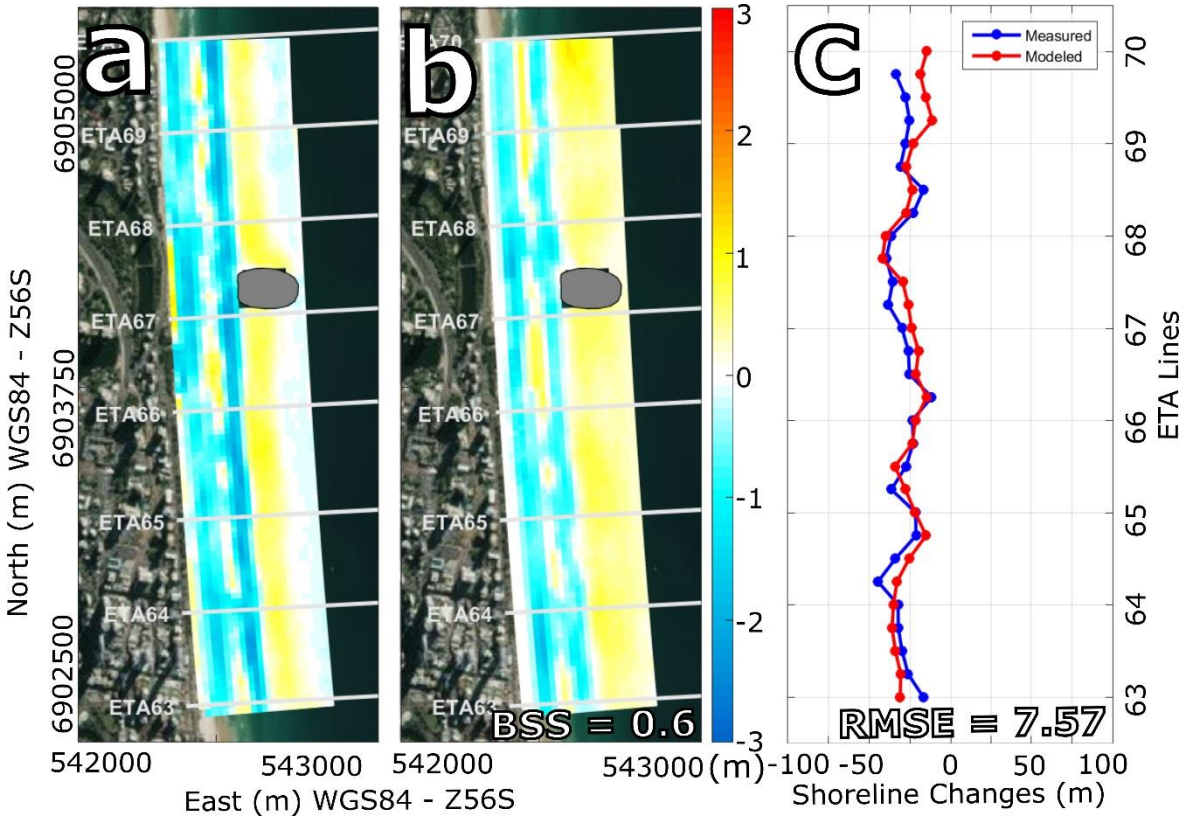


436

437 **Figure 6: Morphological changes between 2nd August 2018 and 12th December 2018. a)**
438 **measured, b) modelled and, c) shoreline changes right - measured (blue) vs modelled**
439 **(red).**

440 *3.2.3 Sediment Transport Scenarios*

441 A calibrated model can be used to assess the regional conditions, providing a bigger picture
442 of conditions when compared to the single study site location measurements. The calibrated
443 model can also be used to simulate scenarios that were not observed during the
444 measurements. Figure 7 presents the waves, currents and sediment transport for median
445 waves from northeast (Figure $7_{a\text{-}c}$), east (Figure $7_{d\text{-}f}$), and southeast (Figure $7_{g\text{-}i}$) over an
446 accreted beach simulated at mean sea level (a water level of 0 m AHD). Similarly, Figure 8
447 presents the results for extreme waves over an accreted beach simulated at mean sea level
448 (refer to supplementary material for eroded beach results). Note that the scales for median
449 and extreme waves are different for $H_s$ (1.5 m for median - Figure 7 - and 4 m for extreme -
450 Figure 8) and they differ by one order of magnitude for sediment transport (median: O $10^{-4}$
451 $m^3/s/m$, extreme: O $10^{-3}$ $m^3/s/m$). Results for low and high tides as well as waves from north
452 and south are provided in the supplementary material.

453 Under median conditions, sediment transport is generally observed along the inner bar
454 (Figure 7). The steepening of the waves is observed over the reef and the waves are
455 focused inshore between ETA 67 (waves from northeast, Figure $7_c$) and to the south of ETA

68 under southeasterly waves (Figure $7_{i}$). Easterly waves (Figure $7_{d-f}$) tend to create circulation cells along the study area with increased currents around the reef (towards the shore over the reef, deflecting offshore north and south of the reef). Low oblique waves generate alongshore currents that are deflected offshore as they pass the reef, where the sediment transport reduces. The results presented also reinforce the influence of the bar morphodynamic state (antecedent condition) on the development of current patterns and the associated sediment transport.

While waves from north and northeast transport sand to the south and waves from southeast and south transport sand to the north, easterly waves tend to present low net longshore transport even under extreme scenarios (Figure $8_{d-f}$) with the transport direction often associated with circulation cells. Extreme waves from northeast (Figure $8_{a-c}$) and southeast (Figure $8_{g-i}$) are the most effective directions for sediment transport, extending the transport zone further offshore (700 m seaward of the A-line). Under these conditions Narrowneck reef deflects the longshore current around it whilst reducing the sediment transport on its immediate downdrift side.

The profile condition (eroded/accreted) also has an important role in modulating the sediment transport pathways (see supplementary material). While eroded beaches tend to concentrate most of the sediment transport on the offshore bar (see supplementary material), accreted beaches tend to distribute the sediment transport more evenly across the surf zone. Similarly, the modeled total transport along the cross-sections changes with the

water levels - during high tides, it is shifted shoreward while during low tides it shifts seaward (see supplementary material).

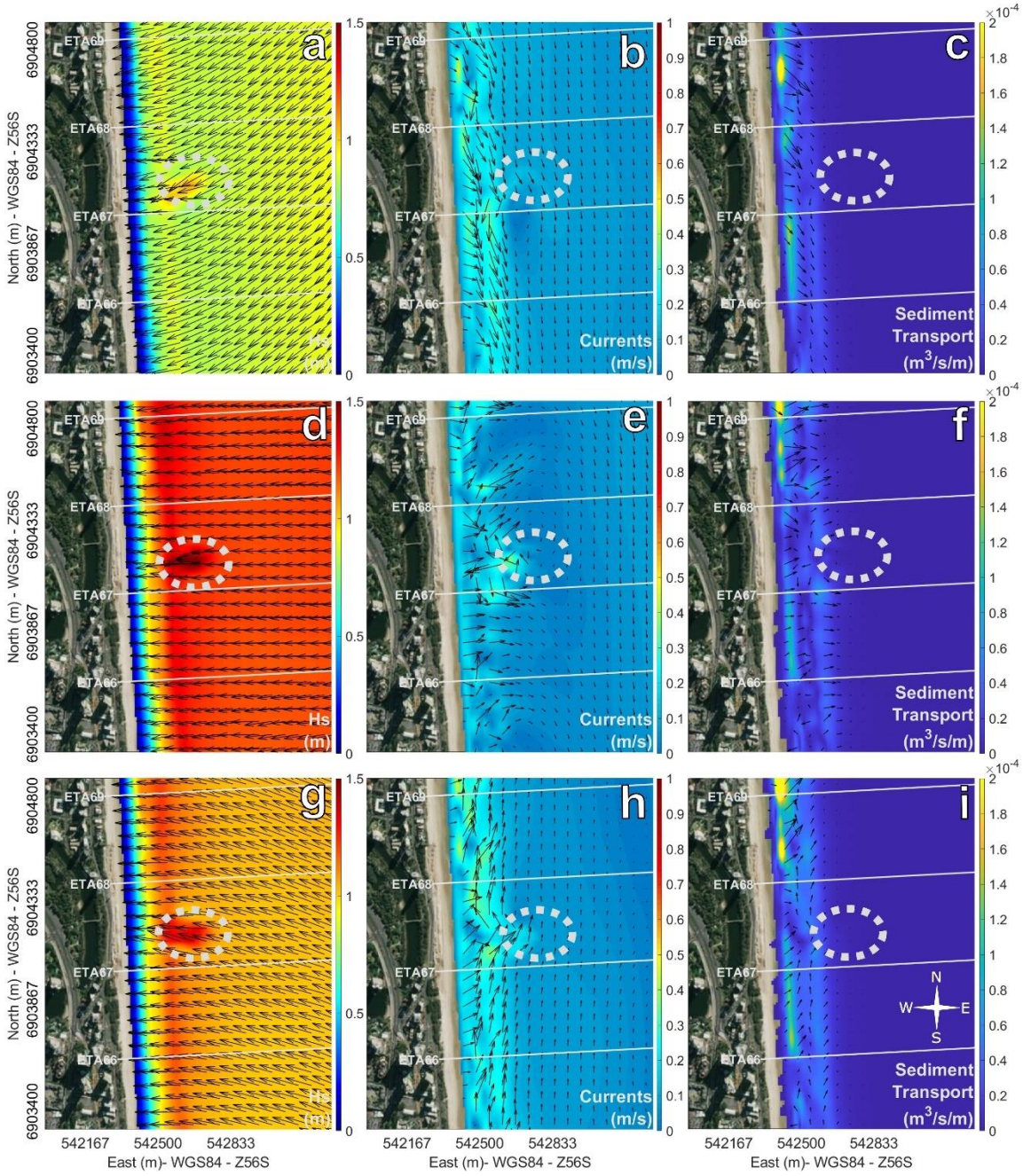


**Figure 7: Numerical model results (Delft 3D). Waves (left), currents (centre) and sediment transport (right) under median northeast (a-c), east (d-e) and southeast (g-i) wave incidence over an accreted beach condition. Ellipse indicates the approximate location of the MPAR.**

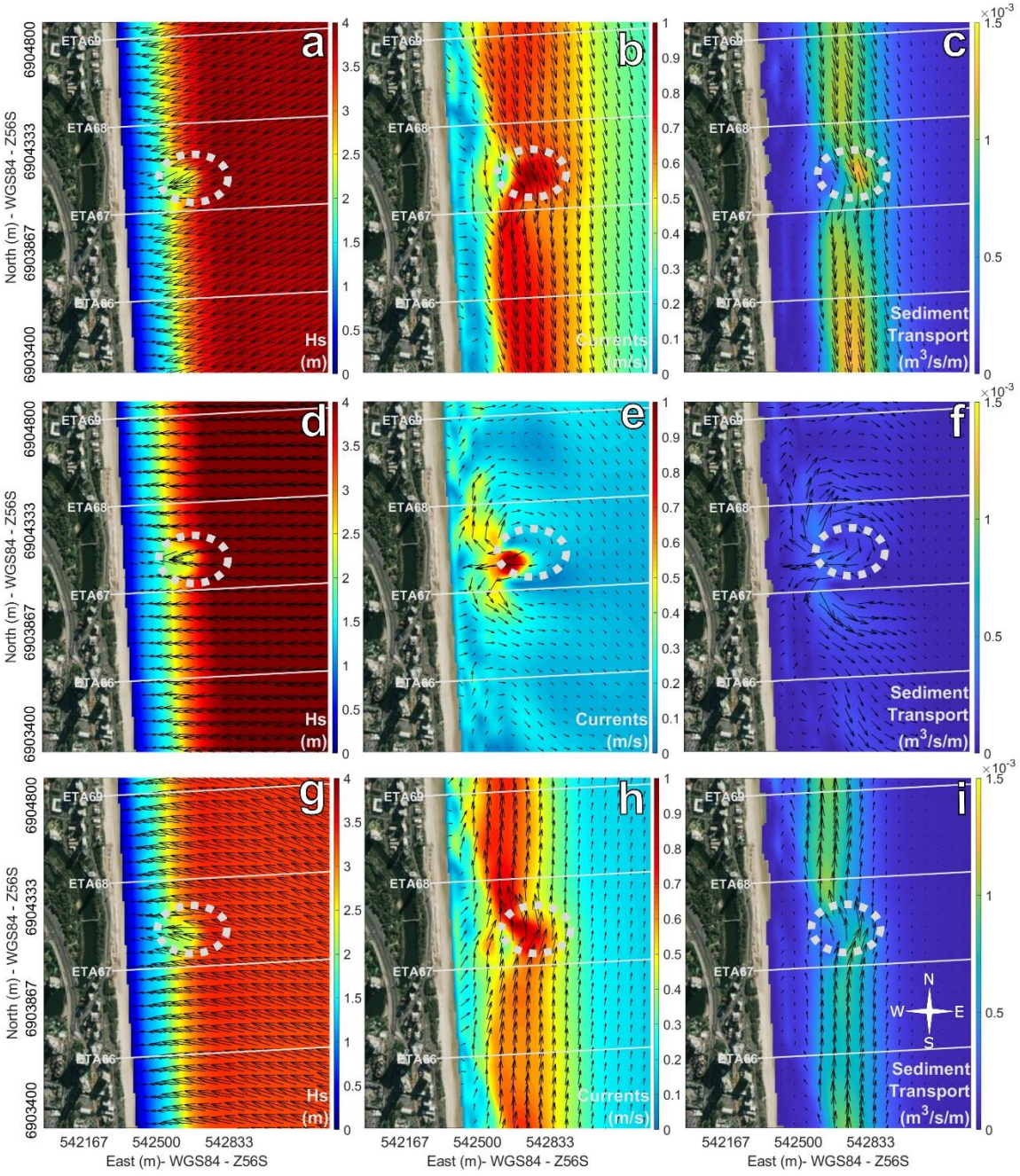


483

484 **Figure 8: Numerical model results (Delft 3D). Waves (left), currents (centre) and**
485 **sediment transport (right) under extreme northeast (a-c), east (d-e) and southeast (g-i)**
486 **wave incidence over an accreted beach condition. Ellipse indicates the approximate**
487 **location of the MPAR.**

488 **4 DISCUSSION**

489 The results presented here were divided into two main components: high resolution topo-
490 bathymetric surveys and, numerical modelling. The field data captured the morphological
491 changes in the nearshore encompassing a period of beach recovery followed by two large
492 events and a second recovery period. Numerical modelling was then used to identify the

sediment pathways and understand how the MPAR influences the transport. The analysis of the results indicated that in the short-term, Narrowneck reef locally impacts the surrounding morphological changes by changing the sediment transport pathways and creating circulation cells and shadow zones within the longshore current, where sand deposits, helping to protect the coastline in the lee of the structure.

While the topo-bathymetric surveys provide a reliable representation of the bar morphology, capturing such data is time-consuming, resource intensive and weather dependent, thus, regular temporal spacing of these types of surveys are rare in the literature (e.g. de Schipper et al., 2016; Murray et al., 2019; Vidal-Ruiz and Alegria-Arzaburu, 2020). Moreover, conditions that are not captured by the surveys can be analysed with modelling demonstrating that these complementary methods are very useful to understand the sediment pathways around MPARs. A calibrated model was capable of reproducing the waves and currents (Figure 5) as well as the morphological changes (Figure 6) around the reef area. The model presented low RMSE values for waves and currents and a reasonable/good morphological calibration with sedimentation patterns that were well related to the measurements. Patterns of erosion and sedimentation as well as the shoreline position (Figure 6) show that the model can reliably simulate the nearshore processes which are particularly useful to complement the topo-bathymetric dataset collected in the area.

With an accreted profile the sediment transport pathways tend to be more evenly distributed across the profile. The sediment transport pathway for eroded profiles however, tended to be more concentrated upon the shore-detached bar, with the majority of transport occurring under higher wave energy (see supplementary material). Under lower waves (that do not break over the bar or the reef), the longshore transport tended to be higher over eroded profiles compared to accreted profiles as less dissipation occurs due to reduced bottom friction (refer to supplementary material sediment transport figures under different beach conditions).

Five main patterns of morphological change and sediment pathways have been observed in the measured dataset and are supported by the numerical modelling:

1) the reef can act by focusing waves inshore, particularly under lower waves (Figure 7). While this wave focusing may be beneficial for the secondary goal of the reef improving surfing inshore of the reef (Jackson et al., 2007) it could, depending on conditions, create a localised erosion point (particularly if waves persist from the same direction for long periods of time). Typically though, conditions leading to this outcome do not last long due to considerable variability in wave direction (continuously changing the focusing point) and the recurrence of wave obliquity that tends to straighten the shoreline (Price et al., 2013; Garnier

et al., 2013). The same factors may also explain the absence of a persistent shoreline salient in the dataset;

2) during large easterly waves a net offshore transport is observed (Figure $3_5$, Figure $4_d$), with a slightly higher erosion rate observed inshore of the reef compared with areas to the north and south of the reef. This observation is due to the area inshore of the reef receiving higher sediment deposition prior to the high energy easterly event and is probably exacerbated by the circulation cells formed by the wave breaking over the reef under these conditions (Figure $8_{d\text{-}f}$). These types of surf zone circulation cells have been numerically predicted by Ranasinghe et al. (2006) who demonstrated the importance of the distance of the structure from shore on the development of the cell circulation. Additionally, this has been observed in natural reefs (Nemes et al., 2019);

3) under oblique waves a longshore current develops and the reef acts to deflect these currents seaward of the reef on the downdrift side, creating a shadow zone where sediment deposition occurs (Figure $3_5$). Narrowneck reef was designed to act as a holding point for the longshore sediment transport, however, the positive impact it has on deflecting the current (offshore) and creating a shadow zone where the sand deposition was not initially predicted. The deflection of currents due to the presence of obstacles to the longshore currents has been reported in the literature by modelling and measurements (e.g. Vieira da Silva et al. 2016, 2020) and was observed in the initial modelling phase of Narrowneck (Black, 1999), however it was linked to a potential erosion area around the northwest part of the reef rather than the sedimentation area observed by this study. Nearshore currents are also strongly linked to morphological changes, facilitating deposition where the currents reduce speed. Near MPARs, these sand deposits would, in turn, act to further dissipate wave energy, aiding in the MPAR's aim of coastal protection;

4) as the reef-aligned offshore bar begins to migrate onshore a deeper area is formed just inshore of the reef (Figure $3_{7\text{-}9}$). This localised trough or depression forms as a result of the lack of sand locally available to migrate onshore due to the presence of the reef. This depression eventually dissipates in the net direction of the longshore drift (north) and does not appear to have an impact on the shoreline (Figure $4_j$);

5) the MPAR also acts as a stabilising point for the offshore bar as it moves onshore in a crescentic shape (Figure $3_{10}$). Subsequently, there is a downdrift offset (seaward) of the inner bar due to the oblique waves incidence, similar to findings presented by Price et al. (2013).

Vieira da Silva et al. (2020) showed that the beach and bars in the region of the MPAR have evolved with increased sedimentation in the updrift side. The data presented here showed a

localised effect of the reef on the morphology with limited impact on the shoreline which indicated the re-establishment of the longshore sediment transport as was initially predicted (Black, 1999; Turner et al., 2001). While high frequency video monitoring of the study site has not captured the influence of the MPAR on the cross-shore movement of the nearshore bars (Bouvier et al., 2019), an increased volume of sand on the reef's updrift side has previously been identified in the mid- to long-term (Vieira da Silva et al., 2019, 2020). This finding is supported by the short-term data presented in this study where the surveys (see supplementary material) indicate that the bar crest at survey line ETA 67 (updrift) is consistently shallower than at ETA 68 (downdrift), except when sand accumulates on the north side of the reef driven to the shadow zone by the deflection of longshore currents, locally increasing the bar crest. Twenty years after Narrowneck reef construction, the MPAR has shown a localised effect on the nearshore morphology that helps to maintain the beach in a similar state compared to the adjacent areas whereas it was previously more vulnerable (i.e. a hotspot). Sediment transport pathways are shown to occur both inshore and offshore of the reef, under varying hydrodynamic and morphodynamic conditions. This study has identified scenarios whereby a previously unforeseen deposition of sand downdrift of the reef occurs in the sub-tidal region. Numerical modelling and in-situ field data indicate that this deposition is caused by the deflection of the longshore currents around the reef and the creation of a shadow zone adjacent to the MPAR.

This deposition process, associated with the presence of the MPAR, aids in coastal protection by dissipating incoming wave energy, before it reaches the shoreline and provides a temporary sediment store to feed the downdrift areas (Figure $3_{6\text{-}8}$) in a process that is akin to headland sand bypassing (Short and Masselink, 1999; Klein et al, 2020) and moreover, it is closely linked to the wave height and direction (Vieira da Silva et al., 2018b). This is likely the reason why the downdrift erosion expected during design phase (Turner et al, 2001) has not been observed in the data.

To date, only a few MPARs have been constructed (Mead and Black, 1999; Black, 2001; Taranaki Regional Council, 2009; Atkins, 2010; Mead et al., 2010; Yardley et al., 2012; Mortensen et al, 2015) with some reporting failures and all generally considered to underperform in at least one aspect of their design. Twenty years after construction of the world's first MPAR (i.e. Narrowneck reef), there is still much knowledge to be gained from the study of these nearshore coastal protection structures in terms of their performance outcomes and interaction with sediment transport pathways. This has been acknowledged by many authors and the discussion and construction of new similar structures is increasing in the literature (e.g. Mortensen et al, 2015; López et al, 2016; Lee et al., 2018; Antunes do Carmo, 2019). To inform the construction of future coastal protection structures, the

monitoring and modelling of existing MPARs that have been in place for several years is crucial for progress and is lacking in peer-reviewed journals. This study represents the first post-construction quantification of the sediment transport and detailed morphological changes influenced by a MPAR based on a combination of topographic surveys and numerical modelling two decades after the MPAR construction.

Considering future predicted wave climate change scenarios (Hemer et al., 2013; Wang et al., 2014; Camus et al., 2017; Young and Ribal, 2019) coastal erosion is likely to increase in many areas that were previously considered to be stable. While relocating coastal cities can be very challenging (Abel et al., 2011), the use of coastal protection strategies still appears as a feasible solution. These will most likely include traditional solutions such as groynes, seawalls and beach nourishment, however, the use of multi-purpose artificial structures may be considered.

This paper presented the short-term morphological response of a vulnerable sandy open coastline to the presence of a MPAR for a range of commonly experienced wave-climate conditions. This research was underpinned by in-situ field data collected in a highly dynamic surf zone and a calibrated numerical model to contribute to a better understanding of the sediment transport pathways and morphological changes in a full-scale, existing structure two decades after construction. The morphodynamic processes influenced by the MPAR identified in this study will contribute to a better understanding of sediment pathways and morphological changes around such structures.

## 5. CONCLUSIONS

Most of the information on MPAR design and monitoring to date has been published in technical reports and conference papers. This limits the broader international knowledge base on design outcomes for MPARs for the scientific and coastal management community. Publication in peer-reviewed journals is very important to the growth of this science and to inform future works. In addition, the published literature regarding design and conditions prior to construction of the existing MPARs is significantly higher than post-construction monitoring and performance literature despite the importance of the assessment of long-term monitoring and data to better understand the actual response without the assumptions and simplifications intrinsic of modelling with limited calibration data. This is probably due to a primary focus on capital works, logistics and budgets following construction, a lack of, or under-reported monitoring programs and data availability to the scientific community. This highlights the importance of continuing monitoring and reporting in the literature of these novel structures to better understand the influence that different interventions have on the

localised longshore transport and the resulting effects on beach morphology and coastal infrastructure protection.

Twenty years after construction, the Narrowneck reef site has more sand deposited updrift and the longshore transport seems to have re-established with minimal impacts on the upper beach. The location of the reef within the active surf zone worked as planned allowing sand to bypass inshore of the reef, particularly under modal wave conditions. Although not initially expected, the results presented in this work demonstrate that the sand bypassing can also occur offshore of the structure under certain conditions (large oblique waves). Whilst a persistent salient at the shoreline inshore of the reef was not observed in the dataset presented here, Narrowneck reef evidently does affect the sediment transport and morphological changes in the short-term, helping to sustain the overall medium to long-term increased volume of sand (due to large scale nourishment campaigns) while allowing sand to also bypass the reef and continue downdrift without significant negative impacts.

Low (e.g. $H_s$ lower than approximately 1.5 m) shore-normal waves are focused inshore of the reef and rarely produce localised erosion due to the natural variability of the wave direction that continuously shifts the enhanced energy point along the beach. Furthermore, under oblique waves a longshore current is formed which tends to straighten the shoreline and bar(s). During calmer conditions, the offshore bar migrates onshore, and the reef may act as a holding point for the surf zone bar helping to maintain the beach in the lee of the reef, as waves dissipate over the reef and the adjacent bar. During this onshore movement of the bar, a local depression has been observed inshore of the reef due to the lack of shoreward sand supply at that location, however this feature is readily dissipated alongshore and does not seem to impact the shoreline.

Large (e.g. $H_s$ higher than approximately 1.5 m) shore-normal waves tend to transport sand offshore and generate circulation cells as the waves break over the reef. More oblique waves, on the other hand, develop a longshore current that is deflected as it passes the reef, reducing speed immediately downdrift of the structure and favouring sand deposition at this location. As can be seen in the data and modelling this sand deposit may act as a temporary stock (source) of sediment (for the downdrift). This is a novel result, which has not been observed in other MPARs or previously predicted, moreover a direct process has not been suggested until now.

The short-term morphological response to the MPAR after two decades is more closely related to the deflection of longshore currents as they encounter the reef than to the dissipation of wave energy, mainly because MPARs are designed to dissipate just enough wave energy so that the wave can still be surfed.

**Acknowledgement**

This research project was sponsored by the City of Gold Coast (the City) through a funding and collaboration agreement between the City and Griffith University. The City has provided data, including bathymetric survey, and project overview to assist in the understanding of this research topic and its benefit to the City. The authors also would like to thank the Queensland Government for providing data, the students, interns and volunteers that helped during the fieldwork campaigns and the constructive feedback from the anonymous reviewer.

**References**

Abel, N., Gorddard, R., Harman, B., Leitch, A., Langridge, J., Ryan, A., Heyemga, S., 2011. Sea level rise, coastal development and planned retreat: analytical framework, governance principles and Australian case study. *Environmental Science & Policy*. 14(3), 279-288.

Antunes do Carmo, J.S., 2019. The changing paradigm of coastal management: The Portuguese case. *Science of the Total Environment*. 695, 133807. https://doi.org/10.1016/j.scitotenv.2019.133807

ATKINS, 2010. Borth Coastal Defence Scheme – Environmental Statement Non-Technical Summary. Report 5037097-830/62/DG/019. 48 pp.

Beaman, R.J., 2010. Project 3DGBR: A high-resolution depth model for the Great Barrier Reef and coral sea. Marine and Tropical Sciences Research Facility (MTSRF) Project 2.5i.1a Final Report, MTSRF, Cairns, Australia, pp. 13 plus Appendix 1. Available at: http://www.deepreef.org/images/stories/publications/reports/Project3DGBRFinal_RRRC2010.pdf

Black, K. and Mead, S., 1999. Design of surfing reefs. *Reef Journal*, 1(1), 177-191.

Black, K., 1999. Designing the shape of the Gold Coast Reef: sediment dynamics. Proceedings of the Coasts & Ports '99 Conference, 14-16 April 1999, Perth, Australia. Vol 1, pp.58-63.

Black, K. and Mead, S., 2001. Design of the Gold Coast reef for surfing, public amenity and coastal protection: surfing aspects. *Journal of Coastal Research*, SI 29, 115-130. ISSN 0749-0208.

Black, K., 2001. Artificial surfing reefs for erosion control and amenity: Theory and application. *Journal of Coastal Research*. SI 34. 1-14. ISSN 0749-0208

Blacka, M.J., Shand, R.D., Carley, J.T., Mariani, A. A review of artificial reefs for coastal protection in NSW. *WRL technical report 2012/08*. June, 2013. 130pp.

Boak, L., McGrath, J., Jackson, L.A., 2000. IENCE — A Case Study — The Northern Gold Coast Beach Protection Strategy. Proceedings of the 27th International Conference on Coastal Engineering. 16 to 21 July 2000, Sydney, Australia. https://doi.org/10.1061/40549(276)289

Booij, N., R. Ris and L. Holthuijsen, 1999. A third-generation wave model for coastal regions, Part I, model description and validation. *Journal of Geophysical Research* 104 (C4): 7649-7666. https://doi.org/10.1029/98JC02622

Bouvier, C., Castelle, B., Balouin, Y., Splinter, K.D., Blacka, M., Bubarbier, B., 2019. Cross-shore sandbars response to an artificial reef: An intersite comparison. Proceedings of the 9th international conference on Coastal Sediments, 2019, Tampa/St. Petesburg, USA, May, 2019. https://doi.org/10.1142/9789811204487_0137

Camus, P., Losada, I. J., Izaguirre, C., Espejo, A., Menéndez, M., and Pérez, J., 2017. Statistical wave climate projections for coastal impact assessments, *Earth's Future*, 5, 918–933, doi:10.1002/2017EF000609

Castelle, B., Turner, I.L., Bertin, X., Tomlinson, R., 2009. Beach nourishment at Coolangatta bay over the period 1987–2005. *Coastal Engineering*.56, pp.940-950. https://doi.org/10.1016/j.coastaleng.2009.05.005

Correa, I.D., Gonzalez, J.L., 2000. Coastal erosion and village relocation: A Colombian case study. *Ocean and Coastal Management*. 43(1), 51-54. https://doi.org/10.1016/S0964-5691(99)00066-6

Garnier, G., Falqués, A., Calvete, D., Thiébot, J., Ribasm F., 2013. A mechanism for sandbar straightening by oblique wave incidence. *Geophysical Research Letters*. 40, 2726-2730. doi:10.1002/grl.50464

Grace, B., Thompson, C., 2020. All roads lead to retreat: adapting to sea level rise using a trigger-based pathway. *Australian Planner*. https://doi.org/10.1080/07293682.2020.1775665

Greenslade,D., Hemer, M., Babanin, A., Lowe, R., Turner, I., Power, H., Young, I., Ierodiaconou, D., Hibbert, G., Williams, G., Aijaz, S., Albuquerque,J., Allen, S., Banner, M., Branson, P., Buchan, S., Burton, A., Bye, J., Cartwright, N., Chabchoub, A., Colberg, F., Contardo, S., Dufois, F., Earl-Spurr, C., Farr, D., Goodwin, I., Gunson, J., Hansen, J., Hanslow, D., Harley, M., Hetzel, Y., Hoeke, R., Jones, N., Kinsela, M., Liu, Q., Makarynskyy, O., Marcollo, H., Mazaheri, S., McConochie, J., Millar, G., Moltmann, T., Moodie, N., Morim, J., Morison, R., Orszaghova, J., Pattiaratchi, C., Pomeroy, A., Proctor, R., Provis, D., Reef, R., Rijnsdorp, D., Rutherford, M., Schulz, E., Shayer, J., Splinter, K., Steinberg, C., Strauss, D., Stuart, G., Symonds, G., Tarbath, K., Taylor, D., Taylor, J., Thotagamuwage, D., Toffoli,

735 A., Valizadeh, A., van Hazel, J., Vieira da Silva, G., Wandres, M., Whittaker, C., Williams, D.,
736 Winter, G., Xu, J., Zhong, A. and Zieger, S., 2020. 15 priorities for wind-waves research: An
737 Australian perspective. *Bulletin of the American Meteorological Society*. Vol. 101, No. 4.
738 doi.org/10.1175/BAMS-D-18-0262.1

739 Hemer, M. A., Fan, Y., Mori, N., Semedo, A., and Wang. X. L., 2013. Projected changes
740 wave climate from a multi-model ensemble. *Nature Climate Change*. 3, 471–476,
741 doi:10.1038/NCLIMATE1791

742 Hutt, J.A.; Black, K.P.; Jackson, A. and McGrath, J., 1999. Designing the Shape of the Gold
743 Coast Reef: Field Investigations. Proceedings of the Coasts & Ports '99 Conference, 14-16
744 April 1999, Perth, Australia. 1,.299-304.

745 Jackson, A., 2001. Special construction requirements for artificial surfing reefs. *Journal of*
746 *Coastal Research*, SI(29), 147-150. ISSN 0749-0208

747 Jackson, L. A., Corbett, B., 2007. Review of existing multi-functional artificial reefs.
748 Proceedings of the Australasian Conference on Coasts and Ports, 2007.

749 Jackson, L. A., Corbett, B., Tomlinson, R., McGrath, J., & Stuart, G., 2007. Narrowneck reef:
750 review of 7 years of monitoring results. *Shore & Beach*, 75(4), 67-79.

751 Jackson, L. A., Hornsey, W.P., 2002. Engineering and artificial reef. *Geotechnical Fabrics*
752 *Report*. 20(4), 18-25.

753 Jackson, A., Tomlinson, R., Corbett, B., & Strauss, D., 2012. Long term performance of a
754 submerged coastal control structure: a case study of the Narrowneck multi-functional
755 artificial reef. *Coastal Engineering Proceedings*, 1(33), structures.54.
756 doi:10.9753/icce.v33.structures

757 Kamphuis, J.W., 2010. Introduction to coastal engineering and management. *Advanced*
758 *Series on Ocean Engineering*, 2nd ed. Vol 30. World Scientific Press, Singapore (525p).
759 https://doi.org/10.1142/7021

760 Klein, A., Vieira da Silva, G., Taborda, R., da Silva, A., Short, A., 2020. Headland bypassing
761 and overpassing: Form, processes and applications. In: Jackson, D. and Short, A. Sandy
762 *Beach Morphodynamics*. Elsevier, 2020. https://doi.org/10.1016/B978-0-08-102927-5.00023-
763 0

764 Kobashi, D., Strauss, D., Tomlinson, R., 2014. Changing coastlines and processes. In:
765 BURTON, P. (Ed.), Responding to Climate Change: Lessons from an Australian Hotspot.
766 Gold Coast. CSIRO Publishing. DOI: 10.1071/9780643108622

767 Kraus, N.C., 1987. Application of portable traps for obtaining point measurement of sediment
768 transport rates in the surf zone. *Journal of Coastal Research*, 2: 139–152.

769 Lee, M.O., Otake, S., Kim, J.K., Transition of artificial reefs (ARs) research and its prospects.
770 *Ocean and Coastal Management*. 154, 55-65.
771 https://doi.org/10.1016/j.ocecoaman.2018.01.010

772 Lesser, G.R., Roelvink. J.A.; van Kester, J.A.T.M. & Stelling, G.S. 2004. Development and
773 Validation of a Three-Dimensional Morphological Model. *Coastal Engineering*. Vol. 51. P.
774 883-915. https://doi.org/10.1016/j.coastaleng.2004.07.014

775 López, I., Tinoco, H., Aragonés, L., García-Barba, L., 2016. The multifunctional artificial reef
776 and its role in the defence of the mediterranean coast. *Science of the Total Environment.*
777 550, 910-923.

778 Mead, S., Black, K., 1999. A Multipurpose, Artificial Reef at Mount Maunganui Beach, New
779 Zealand. *Coastal Management*, 27:4, 355-365, DOI: 10.1080/089207599263767

780 Mead, S.T., Blenkinsopp, C., Moores, A., Borrero, J., 2010. Design and construction of the
781 Boscombe multi-purporse reef. In: Proceedings of the 32nd International Conference on
782 Coastal Engineering (ICCE), Shanghai, China, July, 2010. 9p.
783 https://doi.org/10.9753/icce.v32.structures.58.

784 Mortensen, S. B., Hibberd, W.J., Kaergaard, K., Kristensen, S.E.,Deigaard, R., Hunt, S.
785 Concept design of a multipurpose submerged control structure for Palm Beach, Gold Coast
786 Australia. In: Australasian Coasts & Ports Conference 2015: 22nd Australasian Coastal and
787 Ocean Engineering Conference and the 15th Australasian Port and Harbour Conference.
788 Auckland, New Zealand: Engineers Australia and IPENZ, 2015: 594-600. ISBN:
789 9781922107794

790 Murray, T., Strauss, D., Vieira da Silva, G., Wharton, C., 2019. Spatial Variability in Beach
791 Morphology with Respect to Wave Exposure Along a Zeta-Shaped Coastline. Proceedings
792 of the 9th international conference on Coastal Sediments, 2019, Tampa/St. Petesburg, USA,
793 May, 2019..https://doi.org/10.1142/9789811204487_0056

794 Nemes, D.D., Criado-Sudau, F.F., Gallo, M.N., 2019. Beach morphodynamic response to a
795 submerged reef. *Water*. 11(2), 340. 1-20. https://doi.org/10.3390/w11020340

796 Ng., K.; Phillips, M.R.; Calado, H.; Borges, P., and Veloso- Gomes, F. 2015. Multifunctional
797 artificial reefs for small islands: An evaluation of amenity and opportunity for São Miguel, the
798 Azores. *Progresses in Geography*. 39(2), 220-257. DOI:10.1177/0309133314567581

Ng., K.; Thomas, T., Phillips, M.R.; Calado, H.; Borges, P., and Veloso- Gomes, F. 2013. Seeking harmony in coastal development for small islands: Exploring multifunctional artificial reefs for Sao Miguel Island, the Azores. *Applied Geography*. 44, 99-111. https://doi.org/10.1016/j.apgeog.2013.07.013

Patterson, D.C., 2007. Sand transport and shoreline evolution, northern Gold Coast, Australia. *Journal of Coastal Research*, SI 50, 147 – 151. ISSN 0749.0208

Patterson, D.C., Nielsen, P., 2016. Depth, bed slope and wave climate dependence of lon g term average sand transport across the lower shoreface. *Coastal Engineering*, 117, 113-125. http://dx.doi.org/10.1016/j.coastaleng.2016.07.007

Pörtner, H.O.; Roberts, D.; Masson-Delmotte, V.; Zhai, P.; Tignor, M.; Poloczanska, E.; Mintenbeck, K.; Nicolai, M.; Okem, A.; Petzold, J. 2019. IPCC Special Report on the Ocean and Cryosphere in a Changing Climate. IPCC Intergovernmental Panel on Climate Change: Geneva, Switzerland.

Price, T. D., B. Castelle, R. Ranasinghe, and B. G. Ruessink, 2013. Coupled sandbar patterns and obliquely incident waves. *Journal of Geophysical Research: Earth Surface.* 118, 1677–1692, doi:10.1002/jgrf.20103

Ranasinghe, R., 2016. Assessing climate change impacts on open sandy coasts: A review. *Earth-science Reviews*. 160, 320-332. http://dx.doi.org/10.1016/j.earscirev.2016.07.011.

Ranasinghe, R., Turner, I., 2006. Shoreline response to submerged structures: A review. *Coastal Engineering*. 53, 65-79. https://doi.org/10.1016/j.coastaleng.2005.08.003

Ranasinghe, R., Turner, I., Symonds, G., 2006. Shoreline response to multi-functional artificial surfing reefs: A numerical and physical modelling study. *Coastal Engineering*. 53, 589-611. doi:10.1016/j.coastaleng.2005.12.004

Ris, R.C., N. Booij and L.H. Holthuijsen, 1999. A third-generation wave model for coastal regions, Part II, Verification, *Journal of Geophysical Research*. C4, 104, 7649-7666. https://doi.org/10.1029/1998JC900123

Roelvink, D., Reniers, A., van Dongeren A., Vries J.T., McCall, R., Lescinski, J., 2009. Modelling Storm Impacts on Beaches, Dunes and Barrier Islands. *Coastal Engineering*. 56 (1133-1152). DOI: 10.1016/j.coastaleng.2009.08.006

de Schipper, M.A., de Vries, S., Ruessink, G., de Zeeuw, R.C., Rutten, J., van Gelder-Maas, C., Stive, M.J.F., 2016. Initial spreading of a mega feeder nourishment: Observations of the Sand Engine pilot project. *Coastal Engineering*. 111, 23-38.

831 Short, A. D. 2000. Beaches of the Queensland coast: Cooktown to Coolangatta: a guide to
832 their nature, characteristics, surf and safety, Sydney, Coastal Studies Unit, University of
833 Sydney. ISBN: 0958650411

834 Short, A.D., Masselink, G. Eds, 1999. Embayed and structurally controlled beaches. In:
835 Short, A.D. (Ed.), Handbooks of Beach and Shoreface Hydrodynamics. John Wiley & Sons,
836 Chichester, UK, 1999; pp. 230–250. ISBN: 978-0-471-96570-1

837 Short, A.D.,Trembanis, A.C., Decadal scale patterns in beach oscillation and rotation
838 Narrabeen Beach, Australia: Time Series, PCA and Wavelet Analysis. *Journal of Coastal*
839 *Research*. 20(2), 523-532. ISSN 0749-0208

840 Sierra, J.P., Casas-Prat, M., 2014. Analysis of potential impacts on coastal areas due to
841 changes in wave conditions. *Climatic Change*. 124, 861–876. doi:10.1007/s10584-014-
842 1120-5

843 Silva, A.P., Vieira da Silva, G., Strauss, D., Murray, T. Woortmann, L. G.,Taber, J.,
844 Cartwright, N., Tomlinson, R,., 2021. Headland bypassing timescales: Processes and driving
845 forces, Science of The Total Environment. 793, 148591.
846 https://doi.org/10.1016/j.scitotenv.2021.148591

847 Simmons, J.A., Harley, M.D., Marshall, L.A., Turner, I.L., Splinter, K.D., Cox, R.J., 2017.
848 Calibrating and Assessing Uncertainty in Coastal Numerical Models. *Coastal Engineering*.
849 125, 28-41. http://dx.doi.org/10.1016/j.coastaleng.2017.04.005

850 Sinay, L., Carter, R.W., 2020. Climate change adaptation options for coastal communities
851 and local governments. *Climate*. 8, 7. doi:10.3390/cli8010007

852 Splinter, K. D., Davidson, M.A., Golshani, A., Tomlinson, R., 2012. Climate controls on
853 longshore sediment transport. *Continental Shelf Research*. 48, 146-156.
854 https://doi.org/10.1016/j.csr.2012.07.018

855 Stuart, G. and Lewis, J., 2011. Gold Coast Shoreline Management Plan – Field
856 Measurements & Data Collection. Technical Report 43800441. 35 pp.

857 Sutherland, J., Peer, A.H., Soulsby, R.L., 2004. Evaluation the Performance of
858 Morphological Models. *Coastal Engineering* 51, 917-939.
859 doi:10.1016/j.coastaleng.2004.07.015

860 Taranaki Regional Council. Technical report for Opunake artificial reef monitoring
861 programme: 2005– 2009. Taranaki Regional Council, September, 2009.

Toimil, A., Losada, I.J., Nichols, R.J., Dalrymple, R.A., Stive, M.J.F., 2020. Addressing the challenges of climate change risks and adaptation in coastal areas: A review. *Coastal Engineering*. 156, 103611. https://doi.org/10.1016/j.coastaleng.2019.103611

Tomlinson, R.B., Jackson, L.A., Bowra, K., 2016. Gold Coast seawall: Status investigations and design review. Journal of Coastal Research. SI 75, 715-719.

Turner, I.L., Aarninkhop, S.G.J., Dronkers, T.D.T., and McGrath, J., 2004. CZM applications of Argus coastal imaging at the Gold Coast, Australia. Journal of Coastal Research., 20(2), 439-452. ISSN 0746-0208

Turner, I.L.; Leyden, V.M.; Cox, R.J.; Jackson, L.A., and McGrath, J.E., 2001. Physical model study of the Gold Coast artificial reef. *Journal of Coastal Research*, SI 29, 131-146. ISSN 0749-0208

van Rijn, L. C., J. A. Roelvink and W. T. Horst, 2000. Approximation formulae for sand transport by currents and waves and implementation in DELFT-MOR. Tech. Rep. Z3054.40, WL |Delft Hydraulics, Delft, The Netherlands.

Van Rijn, L.C., 2011. Coastal erosion and control. *Ocean and Coastal Management*. 54 (12), 567-887. https://doi.org/10.1016/j.ocecoaman.2011.05.004

van Rijn, L.C., Walstra, D.J.R., Grasmeijer, B., Sutherland, J., Pan, S., Sierra, J.P., 2003. The Predictability of Cross-Shore Bed Evolution of Sandy Beaches at the Time Scale of Storms and Seasons Using Process-Based Profile Models. *Coastal Engineering* 47, 295-327. https://doi.org/10.1016/S0378-3839(02)00120-5

Vidal-Ruiz, J. and Alegría-Arzaburu, A.R., 2020. Modes of onshore sandbar migration at a single-barred and swell-dominated beach. *Marine Geology*. 426, 106222. https://doi.org/10.1016/j.margeo.2020.106222

Vieira da Silva, G., Hamilton, D., Murray, T., Strauss, D., Shaeri, S., Faivre, G., Silva, A.P., Tomlinson, R., 2020. Impacts of a multi-purpose artificial reef on hydrodynamics, waves and long-term beach morphology. *Journal of Coastal Research*, SI 95, https://doi.org/10.2112/SI95-137.1

Vieira da Silva, G., Toldo Jr., E.E., Klein, A.H.F., Short, A.D., and Woodroffe, C.D., 2016. Headland sand bypassing – quantification of net sediment transport in embayed beaches, Santa Catarina Island north shore, southern Brazil, *Marine Geology*. 379, 13-27. DOI: 10.1016/j.margeo.2016.05.008

Vieira da Silva, G.; Murray, T., and Strauss, D., 2018a. Longshore wave variability along non-straight coastlines. *Estuarine, Coastal and Shelf Science.* 212, 318-328. doi.org/10.1016/j. ecss.2018.07.022

Vieira da Silva, G.V.; Toldo, E.E., Jr.; Klein, A.H.D.F.; Short, A.D., 2018b. The influence of wave-, wind- and tide-forced currents on headland sand bypassing– study case: Santa Catarina Island north shore, Brazil. *Geomorphology.* 312, 1–11. https://doi.org/10.1016/j.geomorph.2018.03.026

Vieira da Silva, G.; Strauss, D.; Shaeri, S.; Murray, T.; Tomlinson, R., and Hamilton, D., 2019. Longshore sediment interruption and bypassing of a multipurpose artificial reef – preliminary results. Proceedings of the 9th international conference on Coastal Sediments, 2019, Tampa/St. Petesburg, USA, May, 2019. https://doi.org/10.1142/9789811204487_0236

Vousdoukas, M., Ferreira, O., Almeida, L.P., Pacheco, A., 2012. Toward reliable storm-hazard Forecasts: Xbeach Calibration and its Potential Application in an Operational Early-Warning System. *Ocean Dynamics* 62, 1001-1015. DOI 10.1007/s10236-012-0544-6

Walker, J.R.; Palmer, R.Q.; Kukea, J.K. Recreational surfing on Hawaiian reefs. In Proceedings of the 13th Coastal Engineering Conference, Vancouver, BC, Canada, 10–14 July 1972.

Wang, X. L., Feng, Y., and Swail, V. R., 2014. Changes in global ocean wave heights as projected using multimodel CMIP5 simulations, *Geophysical Research Letters*. 41, 1026–1034. doi:10.1002/2013GL058650

Ware, D., Buckwell, A., Tomlinson, R., Fozwell-Norton, K., Lazarow, N., 2020. Using historical responses to shoreline change on Australia's Gold Coast to estimate costs of coastal adaptation to sea level rise. *Journal of Marine Science and Engineering*. 8, 380. doi:10.3390/jmse8060380

Wright, L.D., Short, A.D., 1984. Morphodynamic variability of surf zones and beaches: a synthesis. Marine Geology 56, 93–118. https://doi.org/10.1016/0025-3227(84)90008-2

Yardley, B., Phillips, D., Mead, S., 2012. The suitability of utilising a flat bottom barge development system for construction of a multi-purpose reef in Kovalam, India. A preliminary design case study. *The Reef Jorunal*. 2. 46-63.

Young, I.R., and Ribal, A., 2019. Multiplataform evaluation of global trends in wind speed and wave height. *Science*. 364 (6440), 548-552. DOI: 10.1126/science.aav9527

- Beach morphodynamic state and tide level influence sediment transport pathways
- Sand bypassing occurs mainly inshore of the structure
- Under large oblique waves, sand bypass can occur offshore of the structure
- Deflection of longshore currents influence morphological response to the reef
- Bar crest is usually higher on the reef’s updrift side compared to downdrift